

Magnetic and electrical properties of $(\text{La}_{1-x}\text{Dy}_x)_{0.7}\text{Ca}_{0.3}\text{MnO}_3$ perovskites

S. M. Yusuf,* K. R. Chakraborty, and S. K. Paranjpe†

Solid State Physics Division, Bhabha Atomic Research Centre, Mumbai 400 085, India

R. Ganguly

Novel Materials and Structural Chemistry Division, Bhabha Atomic Research Centre, Mumbai 400 085, India

P. K. Mishra, J. V. Yakhmi, and V. C. Sahni

Technical Physics and Prototype Engineering Division, Bhabha Atomic Research Centre, Mumbai 400 085, India

(Received 18 April 2003; revised manuscript received 14 July 2003; published 18 September 2003)

The effect of substituting La with Dy in the ferromagnetic perovskite $\text{La}_{0.7}\text{Ca}_{0.3}\text{MnO}_3$ has been studied in the series $(\text{La}_{(1-x)}\text{Dy}_x)_{0.7}\text{Ca}_{0.3}\text{MnO}_3$ ($x=0, 0.114, 0.243, \text{ and } 0.347$). Magnetic and transport properties have been measured using ac susceptibility, dc magnetization, neutron-depolarization, neutron-diffraction, and resistivity techniques. These studies show that an increase in Dy concentration suppresses the low-temperature ferromagnetic ground state, driving the system (for $x=0.114$ and 0.243) first into a randomly canted ferromagnetic state with a reduced metal-insulator transition temperature and then (for $x=0.347$) to an “insulating” cluster-spin-glass state. Such deterioration of ferromagnetism and metallic conduction with Dy substitution is explained on the basis of a decrease in the transfer integral, t_o (describing the hopping of e_g electrons between Mn^{3+} and Mn^{4+} , known as ferromagnetic double-exchange interaction), resulting from an increase in the structural distortion. The randomly canted ferromagnetic state and the cluster-spin-glass state for $x=0.243$ and 0.347 compounds, respectively, have been confirmed by neutron-depolarization measurements. These observed features have been attributed to a competition between the coexisting ferromagnetic double-exchange and the antiferromagnetic superexchange interactions in the distorted structures with reduced geometrical tolerance factor t and the randomness resulting from the random substitutions of La^{3+} with Dy^{3+} .

DOI: 10.1103/PhysRevB.68.104421

PACS number(s): 75.50.Lk, 75.60.Ch

I. INTRODUCTION

In recent years there has been a growing interest in rare-earth manganese perovskites of the type $R_{(1-x)}A_x\text{MnO}_3$, where R denotes the trivalent rare-earth ions and A denotes the divalent alkali-earth-metal ions. This is because they exhibit a range of extraordinary magnetic, electronic, and structural properties including colossal negative magnetoresistance,¹⁻³ charge ordering,⁴⁻⁷ magnetic-field-induced changes in the structure,^{8,9} and the transport properties¹⁰ and also because of their potential technological applications.

When in a perovskite manganite, LaMnO_3 ($T_N=120$ K, Refs. 4 and 5), a divalent ion, A substitutes for a La, a proportional number of Mn^{3+} ions are converted to Mn^{4+} . In the doped state with mixed Mn valence, the hopping of e_g electrons between two partially filled d orbital of neighboring Mn^{3+} and Mn^{4+} ions is facilitated by the orbital overlap $e_g(\text{Mn})-2p_\sigma(\text{O})-e_g(\text{Mn})$ and the strong on-site Hund's coupling between the t_{2g} core spins and the e_g electrons. This interaction, known as double-exchange (DE) interaction,^{11,12} brings about simultaneous onset of ferromagnetic and metallic characters. The competition between the coexisting ferromagnetic double-exchange interaction and the $t_{2g}(\text{Mn})-2p_\pi(\text{O})-t_{2g}(\text{Mn})$ antiferromagnetic superexchange interactions plays an important role in determining the magnetic and transport properties of these doped manganites.^{11,12}

Direct substitution of Mn sites can also probe the magnetic and transport properties in these systems, and many early studies¹³⁻¹⁵ and more recent ones have been made.¹⁶⁻²¹

Generally, substitutions of Mn by various ions, such as the $3d$ metals,^{13-15,19,22-26} or In, Al, Ga or Ge,^{17,18,27-30} drastically lowers the critical temperature T_C of the paramagnetic-ferromagnetic transition and eventually produces insulating state and/or spin-glass-like properties for higher level of substitution.^{20,23-25,27-29} Reasons underlying these features are the combined effects of Mn-site substitution viz., (i) a shifting of the average valence in the Mn-O-Mn network and (ii) changes in the band structure and hence the conduction-electron-mediated DE interaction.³¹ Further Mn-site substitution by nonmagnetic ions such as Ti^{4+} ,^{24,25} In^{3+29} Al^{3+} ,^{17,26-29} and Zn^{2+} ,³² causes magnetic dilution, while replacement by magnetic ions such as Cr,²² Fe,^{14,30,33-35} Co,^{16,20} Ni,¹⁶ or Cu,²⁶ may introduce additional magnetic couplings. Substitution of Mn site may also cause lattice distortions due to changed ionic size. All these effects are generally intertwined and can influence the magnetic and electrical behavior. Considering the complex influences generated by Mn site doping, if one is interested in studying the ionic size effect on the magnetic and transport properties of these $R_{(1-x)}A_x\text{MnO}_3$ perovskites, it is desirable to focus on replacing La^{3+} by a nonmagnetic ion (with 3^+ ionic state) with different radius without changing the effective Mn valency.

Extensive research has been done on metallic, ferromagnetic manganites of the type $\text{La}_{0.7}\text{Ca}_{0.3}\text{MnO}_3$, through doping the La^{3+} sites with trivalent rare earths (Y,^{36,37} Pr,³⁷ Dy,^{38,39} Tb,^{40,41} etc.) of different sizes keeping the fixed Ca concentration (at 0.3) close to an optimum value in relation to the ferromagnetic interaction. These substitutions bring

about strong lattice effects and disorder, and ultimately influence the magnetic and transport properties of these materials. The lattice distortions introduced by La-site disorder influence the ferromagnetic DE couplings by changing the Mn-O-Mn angle and Mn-O bond distance. The competition of the ferromagnetic DE interactions with the antiferromagnetic superexchange interactions, which are less affected by lattice effects, may give rise to magnetically disordered states. Thus, this type of substitution at the R -sites affects indirectly the magnetic couplings between the Mn sites. Phenomenologically, the changes in the magnetic and transport behaviors can be understood in terms of the tolerance factor t for the perovskite structure, i.e., the average ionic size of the La site, $\langle r_R \rangle$, and the La-site size disorder, i.e., the width σ of the distribution of the ions on the La site.^{37,38,42-44} A decreasing $\langle r_R \rangle$ and/or an increasing σ reduces the transition temperature T_C . Beyond a certain range of values, the lattice disorder brings about glassy magnetic states. In these insulating or metallic states, evidence for ferromagnetic clustering has been found.^{36,41} Within a framework of a DE mechanism, an effective e_g electron transfer between the Mn^{3+} and Mn^{4+} ions in these perovskites is given by $t_o \cos(\theta/2)$, where t_o denotes an e_g electron transfer probability when localized t_{2g} spins are parallel and θ represents the angle between two neighboring t_{2g} spins. Therefore, the mobility of electrons in the DE systems can be controlled by varying t_o and/or θ . With diminishing $\langle r_R \rangle$, the Mn-O-Mn bond angles and the e_g electron transfer probability t_o (which are microscopically interrelated) decrease.³⁷

Terai *et al.*³⁸ have investigated the effects of Dy^{3+} substitution in $(\text{La}_{1-x}\text{Dy}_x)_{0.7}\text{Ca}_{0.3}\text{MnO}_3$ by dc magnetization, resistivity, and magnetoresistance studies. The Curie temperature and the associated metal-insulator transition temperature were reported to decrease drastically with the Dy doping. The compounds with $x=0.143$ ($t=0.911$), 0.243 ($t=0.908$), and 0.286 ($t=0.907$) were reported to show reentrant spin-glass (RSG) behavior where the high-temperature insulating paramagnetic state transforms to a ferromagnetic metallic state at relatively lower temperatures and finally transforms to an insulating spin-glass (with a collapse of ferromagnetic ordering) at further lower temperatures. For $x > 0.286$ ($t < 0.907$), only a spin glass insulator phase appears at low temperatures which was compared with the insulator spin glass state reported by Teresa *et al.*⁴³ for the compound $(\text{La-Tb})_{2/3}\text{Ca}_{1/3}\text{MnO}_3$. The spin glass insulator phase observed in $(\text{La}_{1-x}\text{Dy}_x)_{0.7}\text{Ca}_{0.3}\text{MnO}_3$ for $x > 0.286$ was interpreted³⁸ to be different from a ferromagnetic insulator that appears in the compounds containing light rare-earth-metal ions of Pr^{3+} and/or Y^{3+} .

In this paper, we present results on the $(\text{La}_{1-x}\text{Dy}_x)_{0.7}\text{Ca}_{0.3}\text{MnO}_3$ with $x=0$ ($t=0.916$), 0.114 ($t=0.913$), 0.243 ($t=0.908$), and 0.347 ($t=0.905$) using magnetic and transport measurements by ac susceptibility, dc magnetization, and resistivity, which are combined with investigations of the magnetic order at microscopic and mesoscopic length scales from neutron-diffraction and neutron-depolarization techniques, respectively. In these compounds, where magnetic frustration and disorder are present, the nature of the magnetic correlation cannot be unequivocally de-

termined by bulk magnetic measurements.^{35,45} Neutron-diffraction has been employed in order to characterize the long-range magnetic order and its gradual suppression by the substitution. Neutron depolarization technique probes magnetic inhomogeneity on a length scale of several 10 nm up to few μm and thus, helps in establishing the existence of magnetic domains/clusters for $x=0.243$ and 0.347 of Dy substituted samples. The results provide strong evidence of the presence of ferromagnetic correlation in $(\text{La}_{0.757}\text{Dy}_{0.243})_{0.7}\text{Ca}_{0.3}\text{MnO}_3$ and a cluster-spin-glass state in $(\text{La}_{0.653}\text{Dy}_{0.347})_{0.7}\text{Ca}_{0.3}\text{MnO}_3$ in their low-temperature insulating states contrary to what was concluded by Terai *et al.*³⁸ Since the microscopic neutron-diffraction study confirms that the Dy^{3+} does not show magnetic ordering down to 9 K, our experimental results essentially reflect how the $\langle r_R \rangle$ and σ of the La sublattice influence the magnetic order on the different length scales. A preliminary report of the results of ac susceptibility, dc magnetization, resistivity, and room-temperature neutron-diffraction measurements on the $x=0$ and 0.243 samples has been given elsewhere.³⁹

II. EXPERIMENT

Polycrystalline samples with nominal compositions $(\text{La}_{1-x}\text{Dy}_x)_{0.7}\text{Ca}_{0.3}\text{MnO}_3$ ($x=0, 0.114, 0.243, \text{ and } 0.347$) were prepared by solid-state reaction of MnO_2 (Aldrich, 99.9%), CaCO_3 (Aldrich 99%), La_2O_3 (Aldrich 99%), and Dy_2O_3 (Aldrich 99%) at 1250 °C. Stoichiometric amounts of the compounds were mixed together and were first calcined at 1000 °C for 12 h. The calcined products were then sintered at 1300 °C for one week with several intermediate grindings and pelletizations. La_2O_3 was preheated at 1000 °C prior to the reaction. Room-temperature powder x-ray-diffraction patterns confirmed the single-phase formation of orthorhombic perovskite structure.

The real part of ac susceptibility (χ_{ac}) was measured for all the four samples ($x=0, 0.114, 0.243, \text{ and } 0.347$) using an avalanche photodiode (APD) closed cycle helium refrigerator with Meissner coil assembly in conjunction with an EG&G Model 5208 lock-in amplifier. Measurements were performed at a frequency of 80 Hz and in an ac field of 0.5 Oe. dc electrical resistance measurements were performed on the $x=0, 0.243, \text{ and } 0.347$ samples by the standard four-probe method using a Datron (model 1071) multimeter over the temperature range of 14–300 K.

Zero-field cooled virgin dc magnetization measurements were carried out on the $x=0, 0.243, \text{ and } 0.347$ samples at 15 K using a superconducting quantum interference device (SQUID) magnetometer as a function of magnetic field up to 50 kOe. Field cooled dc magnetization measurements were also carried out on the $x=0.243$ sample using the SQUID magnetometer over the temperature range of 5–290 K and in 50 and 500 Oe magnetic field in the heating cycle. All measurements were carried out on compacted powder samples. Compacting ensures that rotation of the crystallites does not take place during measurements.

The one-dimensional (1D) (z - z) neutron-depolarization measurements (a good tool to probe the magnetic inhomogeneity on a mesoscopic length scale⁴⁶⁻⁵⁰) were carried out on

the $x=0.243$ and 0.347 samples using the neutron-polarization analysis spectrometer (PAS) at Dhruva reactor, Trombay ($\lambda=1.205$ Å). The detailed description of the spectrometer has been given in earlier papers.^{51,52} The temperature of sample was varied between 15 and 300 K using a closed-cycle helium refrigerator and controlled to better than 0.1 K. Measurements were performed in the heating cycle in the presence of 7 Oe external field after cooling the sample in the same field of 7 Oe from 300 K to 15 K. The incident neutron beam was polarized along the $-z$ direction (vertically down) with a beam polarization of 98.60(1)%. The polarization of transmitted neutron beam was measured along the $+z$ direction as described in detail in an earlier paper.⁵¹ The powder sample used for the depolarization study was in the form of a pellet of cylindrical dimension. The sample was placed in the neutron beam in such a way that its plane surface xz remains perpendicular to the propagation direction y of the polarized neutron beam. The beam passed through an effective sample thickness of 10 mm. The beam size was restricted with a cadmium slit to keep it within the size of the sample. The external magnetic field of 7 Oe (on the sample) was applied parallel to the incident neutron beam polarization direction $-z$ using a small electromagnet.

The unpolarized neutron powder-diffraction measurements were carried out on the $x=0$, 0.243 , and 0.347 samples at 297 K and 15 K (the lowest possible temperature of measurements) in a cylindrical vanadium sample container using the 1D position sensitive detector based profile analysis diffractometer ($\lambda=1.094$ Å) at Dhruva reactor, Trombay.⁵³ The temperature variation of diffracted intensities of the (110) and (002) Bragg peaks of the $x=0.243$ and 0.347 samples were studied from 15 to 200 K. For the $x=0.114$ sample, the neutron-diffraction patterns were recorded at 297, 200, 100, 50, and 9 K using another one-dimensional position sensitive detector based powder diffractometer ($\lambda=1.242$ Å) at Dhruva reactor, Trombay. The diffraction measurements were carried out on the polycrystalline samples with no external magnetic field.

III. RESULTS AND DISCUSSION

A. ac susceptibility

Figure 1 shows the temperature dependence of the ac susceptibility (χ_{ac}) curve for all the four samples. Magnetic transition temperatures (defined as the point of the steepest slope in the χ_{ac} vs T curve) are found to be 232, 111, 70, and 55 K for $x=0$, 0.114 , 0.243 , and 0.347 samples, respectively, indicating that the substitution of Dy for La leads to a strong decrease in the magnetic ordering temperature. The onset of ferromagnetic ordering for the $x=0$ sample is found to be ~ 251 K, in accordance with the reported value in literature.^{54,55} The temperature variation of χ_{ac} for the $x=0.243$ and 0.347 samples is very much different from that of the ferromagnetic $x=0$ and 0.114 samples. For these higher Dy substituted samples ($x=0.243$ and 0.347), the χ_{ac} curves show cusplike peak at 60 K and 46.5 K for $x=0.243$ and 0.347 samples, respectively. Similar peak shapes have been reported in the χ_{ac} plots at the “spin-glass-like”

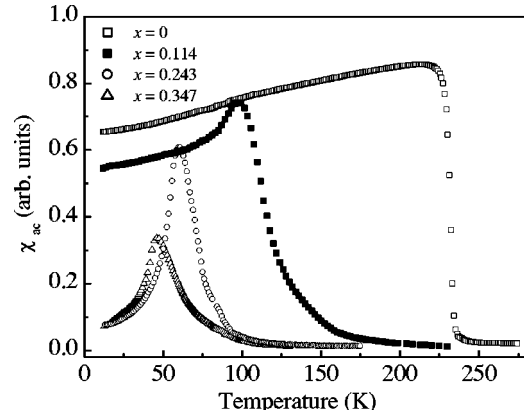


FIG. 1. The temperature dependence of the real part of ac susceptibility for $(\text{La}_{1-x}\text{Dy}_x)_{0.7}\text{Ca}_{0.3}\text{MnO}_3$ samples with $x=0$, 0.114 , 0.243 , and 0.347 .

transition for $\text{La}_{2/3}\text{Ca}_{1/3}\text{MnO}_3$ doped with Ga,⁴⁵ Al,²⁸ In,²⁹ and Fe (Ref. 14) with higher degree of substitution and for the rare-earth site substituted cluster-spin-glass perovskites, such as $(\text{La}_{2/3}\text{Tb}_{1/3})_{2/3}\text{Ca}_{1/3}\text{MnO}_3$ (Ref. 43) and $\text{La}_{0.7}\text{Y}_{0.15}\text{Ca}_{0.3}\text{MnO}_3$.³⁶ Similar χ_{ac} cusps observed for the other perovskites have been ascribed to either a spin-glass-type transition³³ or a local spin canted spin state.³⁵

B. Resistivity

Figure 2 shows the temperature dependence of the resistivity ρ for $x=0$, 0.243 , and 0.347 samples under zero magnetic field. The resistivity curve for $x=0$ sample shows an insulator-metal transition at ~ 240 K with a metallic behavior at lower-temperature side, as reported in the literature.³⁸ For $x=0.243$ sample, the insulator-metal transition temperature shifts to 52 K and the metallic behavior is observed only over the temperature range of 52–35 K, as found by Terai *et*

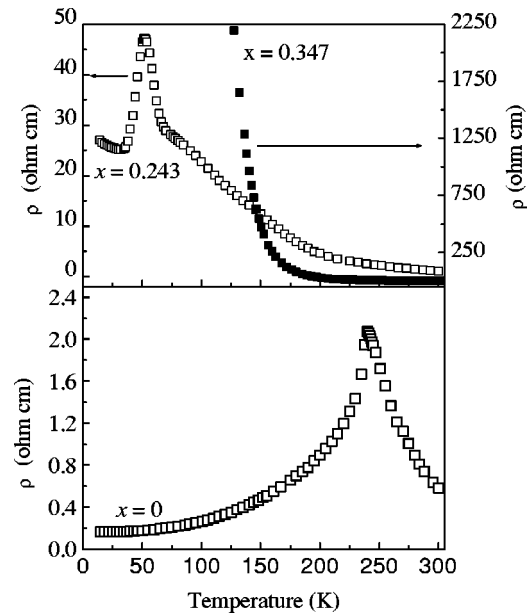


FIG. 2. The zero field resistivity as a function of temperature for $(\text{La}_{1-x}\text{Dy}_x)_{0.7}\text{Ca}_{0.3}\text{MnO}_3$ samples with $x=0$, 0.243 , and 0.347 .

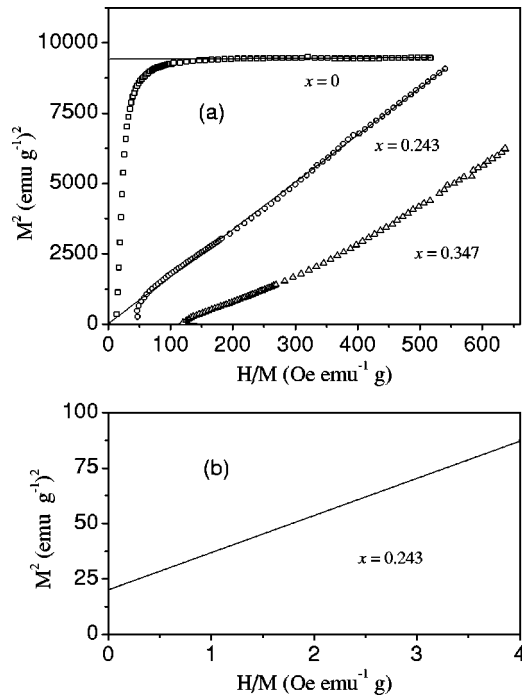


FIG. 3. (a) Arrott plot at 15 K for perovskite compounds with $x=0$, 0.243, and 0.347. Solid lines are the extrapolated lines of the linear fit to the higher H/M data. (b) The extrapolated line of the linear fit to the higher H/M data is enlarged over lower H/M for the $x=0.243$ sample.

*al.*³⁸ At temperatures below 35 K, an insulating behavior reappears. The behavior of resistivity for $x=0.243$ sample is somewhat similar to what was reported for the $(\text{La}_{0.786}\text{Y}_{0.214})_{0.7}\text{Ca}_{0.3}\text{MnO}_3$ perovskite.³⁶ However, the $x=0.347$ compound is found to remain in the insulating state within the range of our measurement capability similar to that observed in the $(\text{La-Tb})_{2/3}\text{Ca}_{1/3}\text{MnO}_3$ perovskite.⁴³

C. dc magnetization

The Arrott plots derived from the zero-field cooled virgin $M(H)$ measurements at 15 K are shown in Fig. 3 for the $x=0$, 0.243, and 0.347 samples. The positive intercept of the straight line extrapolated from the points at high H/M values for the $x=0$ and 0.243 samples on the ordinate clearly indicates the presence of spontaneous magnetization at this temperature (15 K). It is interesting to note that the spontaneous magnetization decreases drastically from 97.08 emu g^{-1} ($=3.69\mu_B$ per formula unit) for the $x=0$ compound to 4.5 emu g^{-1} ($=0.17\mu_B$ per formula unit) for the $x=0.243$ compound; whereas, for the $x=0.347$ sample, no spontaneous magnetization is found, in agreement with the published paper by Teresa *et al.*⁴³ for the insulator spin-glass $(\text{La}_{2/3}\text{Tb}_{1/3})_{2/3}\text{Ca}_{1/3}\text{MnO}_3$. For the $x=0.243$ sample, as discussed later in this paper, the observed value of the spontaneous magnetization $M_S(H=0, T)$ at $T=15 \text{ K}$ ($=4.5 \text{ emu g}^{-1}$) has been used for calculating the magnetic correlation length from the measured neutron depolarization at 15 K.

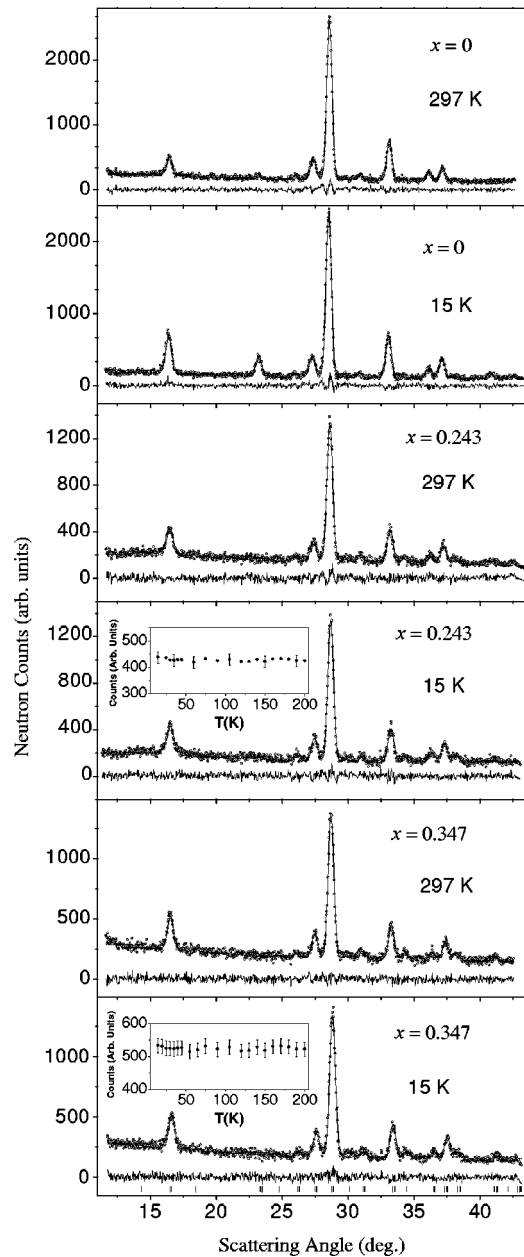


FIG. 4. Observed (open circles) neutron-diffraction patterns ($\lambda = 1.094 \text{ \AA}$) for $(\text{La}_{1-x}\text{Dy}_x)_{0.7}\text{Ca}_{0.3}\text{MnO}_3$ of the $x=0$, 0.243, and 0.347 samples at 297 K and 15 K recorded over the lower angular range where magnetic Bragg reflection intensities, if any, are expected predominantly. The solid lines represent the Rietveld refined patterns. The difference patterns between the observed and calculated patterns are also shown at the bottom of each curve by solid lines. The vertical lines indicate the position of allowed Bragg peaks. The insets show the combined peak intensity of the (110) and (002) inner Bragg peaks ($2\theta \approx 16.6^\circ$) of the $x=0.243$ and 0.347 samples as a function of temperature.

D. Neutron diffraction

Figure 4 shows the observed and Rietveld refined neutron powder diffraction patterns at 15 and 297 K (i.e., well below and above the magnetic transition temperatures) for the samples with $x=0$, 0.243, and 0.347. The patterns are shown only over the lower angular range (scattering angle

$\approx 11\text{--}43$ deg.) where magnetic Bragg reflection intensities, if any, are expected predominantly. The patterns obtained at 15 K and 300 K were analyzed by the Rietveld method using the FULLPROF program.⁵⁶ Refinement shows an orthorhombic perovskite structure (space group $Pbnm$) at all temperatures. For all the samples, the 297-K diffraction patterns could be fitted with only nuclear intensities confirming the paramagnetic nature of the samples at room temperature. Rietveld refinement of data recorded at 15 K shows ferromagnetic ordering for the $x=0$ sample with a net Mn-site ordered moment of $3.42 \pm 0.06 \mu_B$ along the crystallographic c direction as reported in literature.⁵⁴ The moment value obtained in our dc magnetization measurements is in good agreement with these results. However, for both the $x=0.243$ and 0.347 samples, the 15-K diffraction pattern could be fitted with only nuclear intensities confirming the absence of any observable long-range magnetic ordering. For the $x=0.243$ and 0.347 samples, the refinement at 15 K shows a complete absence of ferromagnetic ordered moment with a detection limit^{35,43,45} of $\sim 0.5 \mu_B$ per Mn or Dy site. The absence of any magnetic contribution to the (110) and (002) nuclear Bragg peaks over 15–200 K (shown in inset of Fig. 4) confirms the absence of long-range magnetic order at any intermediate temperatures as well. It may be stressed that no additional Bragg peaks are found either, indicating the absence of any other ordered magnetic phase (antiferromagnetic, spiral, etc.) in the $x=0.243$ and 0.347 samples. The observed low spontaneous magnetization ($=0.17 \mu_B$ per formula unit at 15 K) from the dc magnetization data for the $x=0.243$ sample lies well below the detection limit in the present neutron-diffraction experiments and is, therefore, consistent with the absence of observable ferromagnetic intensity under fundamental Bragg peaks. The absence of observed ordered moment in the neutron-diffraction study for the $x=0.243$ sample suggests that the spins are randomly (local) canted^{35,45} with very large average canting angle of Mn spins. The possibility of uniform canting of spins is ruled out from the absence of any observed magnetic Bragg-peak intensity. The canting of Mn-site moments is, therefore, assumed to be random (local) from site to site so that the ordered component of moments that gives a long-range ferromagnetic ordering over the domain is quite small in magnitude ($\sim 0.17 \mu_B$). A canted ferromagnetic behavior has been reported for other perovskites.^{35,45,57} Such a canted spin model for mixed-valent manganites was theoretically predicted by de Gennes,⁵⁸ within the framework of a model for competing ferromagnetic double-exchange and antiferromagnetic superexchange interactions. For the $x=0.347$ sample the absence of spontaneous magnetization, as also the ordered ferromagnetic moment in the low-temperature neutron-diffraction pattern, might occur due to spin-glass-like ordering.^{43,45} We will discuss later the true nature of the spin ordering in the case of $x=0.243$ and 0.347 samples.

In order to obtain more information on the possible magnetic ordering of the Mn and Dy ions in the Dy-doped samples, we have also recorded neutron-diffraction patterns on a smaller Dy-doped $x=0.114$ compound. Figure 5 shows the observed and Rietveld refined neutron powder-diffraction patterns for the $x=0.114$ sample at 9, 50, 100, 200, and 297

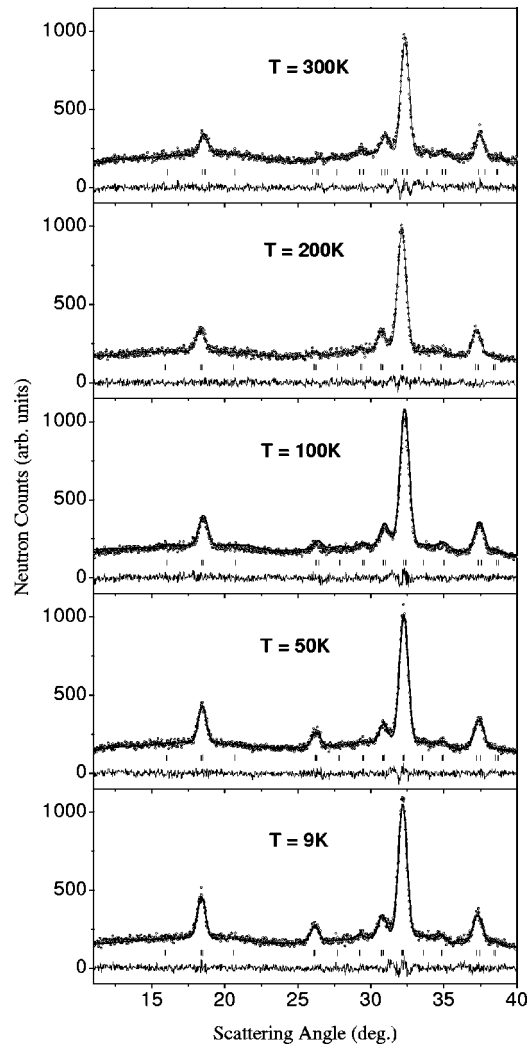


FIG. 5. Neutron-diffraction patterns ($\lambda=1.242$ Å) at several temperatures down to 9 K for $(\text{La}_{0.886}\text{Dy}_{0.114})_{0.7}\text{Ca}_{0.3}\text{MnO}_3$, shown by the open circles. The solid lines represent the calculated patterns. The difference patterns between the observed and calculated intensities are also shown at the bottom.

K over the scattering angular range of $\sim 11\text{--}40$ deg. Refinement confirms an orthorhombic perovskite structure (space group $Pbnm$) at all temperatures. A ferromagnetic ordering of Mn moments with a net Mn-site ordered moment of $3.12 \pm 0.08 \mu_B$ per Mn ion at 9 K, $3.12 \pm 0.13 \mu_B$ at 50 K, and $1.64 \pm 0.18 \mu_B$ at 100 K was found. The ordered Mn moment was found to align along the crystallographic c direction, as in the parent compound. The absence of any ordered moment at 200 and 297 K (above the magnetic ordering temperature 150 K, obtained from our ac susceptibility measurements) confirms the paramagnetic nature of the sample at these higher temperatures. Refinement shows that the Dy moment is not ordered down to 9 K, as found in the dc magnetization study of the $\text{La}_{0.7-x}\text{Dy}_x\text{Sr}_{0.3}\text{MnO}_3$ perovskite.⁵⁹ The reduction of observed site averaged ordered moment for Mn ion in the $x=0.114$ sample (as compared to the parent $x=0$ sample) suggests that the Mn spins are randomly canted at an average angle Φ of ~ 24 deg with respect to the [001] crys-

talline axis in the $x=0.114$ compound. Here, the canting angle Φ is given by the expression, $\cos \Phi = \mu/\mu_0$, where μ ($=3.12\mu_B$) and μ_0 ($=3.42\mu_B$) are the low-temperature ordered moments for $x=0.114$ and 0 samples, respectively.

E. Neutron depolarization

In order to get further clues regarding the nature of spin ordering in the $x=0.243$ and 0.347 samples, we carried out neutron-depolarization experiments and before presenting the results we wish to point out that neutron-depolarization technique is a mesoscopic probe and essentially measures the spatial magnetic inhomogeneity on a length scale, say from 100 \AA to several microns.^{46,47,49} In an unsaturated ferrimagnet or ferromagnet, the magnetic domains exert a dipolar field on the neutron polarization and depolarize the neutrons owing to the Larmor precession of the neutron spins in the magnetic field of domains. A magnetic inhomogeneity on an atomic scale—as in true spin-glass state—has no effect on the neutron polarization. In a true spin-glass phase (in zero-field cooled state), the atomic spins are randomly frozen in space on a microscopic length scale and, as a result, the magnetic induction averages out to zero on a mesoscopic length scale. Hence no depolarization is found in true spin-glass systems. Similarly, no depolarization can be expected in the paramagnetic state because the temporal spin fluctuation is too fast (10^{-12} s or faster) for the neutron-polarization vector to follow the variation in the magnetic field B acting on the moving thermal neutrons. However, one would expect depolarization for the case of clusters of spins (of mesoscopic length scale) with net moments. The domain/spin-cluster size information can therefore be obtained (as an average over the entire sample), and there are essentially no resolution restrictions on the size of the domains which can be measured.

The temperature dependence of the transmitted neutron beam polarization P_f for $x=0.243$ and 0.347 samples with an applied field of 7 Oe are depicted in Fig. 6(a). The procedure of obtaining P_f values from the measured flipping ratios for the transmitted polarized beam is described elsewhere.⁵¹ As shown in the figure, for $x=0.243$ sample, P_f shows a continuous decrease right from ~ 65 K before attaining a constant value below about 28 K. At $T > 65$ K, the value of P_f is the same as that for the incident-beam polarization, implying that this sample is in its paramagnetic phase above 65 K. The magnetic ordering temperature for the $x=0.243$ sample is thus estimated to be about 65 K. The results confirm the presence of domains of spins with net magnetic moments in it. Absence of any evidence of breakdown of domain structure at any temperature below 65 K (which results in a recovery of the transmitted neutron beam polarization P_f) indicates the absence of any transition at temperatures around 35 K, below which an insulating behavior is found, as shown in Fig. 2. Terai *et al.*³⁸ identified the low-temperature phase of the $x=0.243$ sample as the RSG state with ferromagnetic Curie temperature T_C of ~ 57 K and spin-glass transition temperature T_g of ~ 38 K. However, below T_g a collapse of the ferromagnetic ordering was suggested in their report.³⁸ Neutron-depolarization measure-

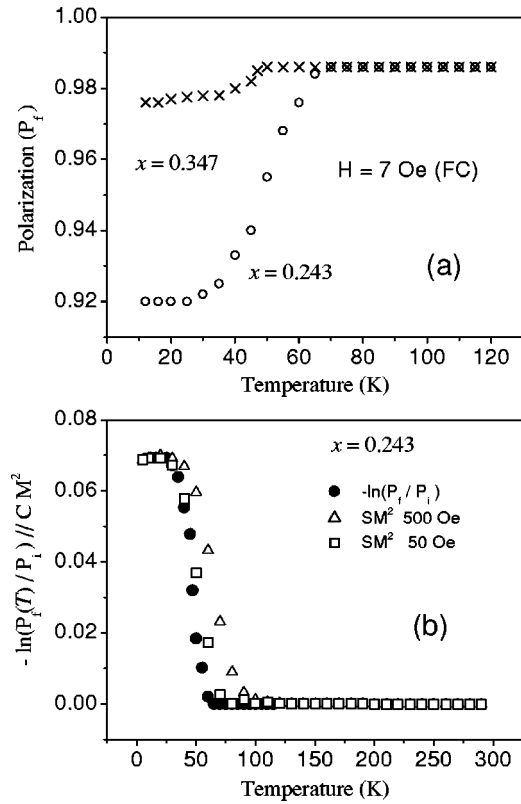


FIG. 6. (a) Temperature dependence of transmitted neutron beam polarization measured at 7 Oe applied field for the $x=0.243$ and 0.347 samples. (b) Comparison of $-\ln[P_f(T)/P_f]$ and $S[M(T)]^2$ at various fields applied during M vs T measurements for the $x=0.243$ sample (see text).

ments performed on several RSG systems, namely, Ni-Mn,⁴⁸ a-Fe-Zr,⁴⁸ a-Fe-Ru-Zr,⁶⁰ a-Fe-Mn,⁶¹ a-Fe-Ni⁶² etc. have shown that long-range ferromagnetic correlation does not breakdown even at $T < T_g$ where some typical spin-glass-like properties are found in macroscopic magnetization measurements. Large ferromagnetic domains of a few micrometers in size do exist at low temperatures, in good agreement with the mean-field predictions. In Ni-Mn system,⁴⁸ ferromagnetic domains were found to exist at all temperatures below T_C even for the samples close to the critical concentration. The compound $x=0.243$ undergoes a spontaneous insulator-metal transition which has a spontaneous ferromagnetic correlation in the metallic state over the temperature range 65–35 K, as expected for the DE-mediated perovskites.³⁵ At $T < 35$ K, too, we observed a ferromagnetic state as reported for the ferromagnetic insulating compounds $(\text{La-Pr})_{0.7}\text{Ca}_{0.3}\text{MnO}_3$ (Ref. 37) and $(\text{La-Y})_{0.7}\text{Ca}_{0.3}\text{MnO}_3$ (Ref. 37) containing light rare-earth-metal ions. The macroscopic magnetic and transport studies of $\text{La}_{0.7-\delta}\text{Y}_\delta\text{Ca}_{0.3}\text{MnO}_3$ (Ref. 36) with $\delta=0.15$ shows a behavior similar to the one observed for the $x=0.243$ sample. However, the low-temperature metallic phase of $\text{La}_{0.7-x}\text{Y}_x\text{Ca}_{0.3}\text{MnO}_3$ with $x=0.15$ was interpreted in terms of cluster glass state³⁶ as against our finding of the randomly canted ferromagnetic phase with large domains ($\sim 5 \mu\text{m}$).

$\text{La}_{0.7-\delta}\text{Dy}_\delta\text{Sr}_{0.3}\text{MnO}_3$ compounds⁵⁹ with δ between 0.35 and 0.4 also show similar magnetization and resistivity behavior as found for the $x=0.243$ sample.

The occurrence of the transverse spin freezing in the RSG state as predicted by the mean-field theory cannot be directly checked by our neutron-depolarization study. This is because the depolarization is mainly determined by the longitudinal spin components.⁴⁸ From the observed depolarization an estimate of the average size of domains/clusters was, however, made using the expression^{47,48,35,45}

$$P_f = P_i \exp\left[-\alpha\left(\frac{d}{\Delta}\right)\langle\Phi_\delta\rangle^2\right], \quad (1)$$

where P_i and P_f are the initial and final neutron beam polarization, α is a dimensionless parameter $\approx 1/3$, d ($= 10$ mm) is the effective thickness of the sample, Δ is the average domain size, and $\Phi_\delta = (4.63 \times 10^{-10} \text{ G}^{-1} \text{ \AA}^{-2}) \lambda B \Delta$ is the precession angle. The internal mean induction $B = 4\pi M_S \rho$ (in Gauss) within a domain at low temperature was estimated from the bulk magnetization measurements. Here M_S is the spontaneous magnetization in emu g^{-1} and ρ is the density of the material in g cm^{-3} . The spontaneous magnetization value of 4.5 emu g^{-1} , obtained from the ‘‘Arrott’’ plot of magnetization at 15 K, has been used for the estimation of B . The mean B of ~ 352 G is obtained using the average sample density of 6.23 g cm^{-3} . Equation. (1) is valid with the assumption that the Larmor precession angle of the neutron spin due to the internal magnetic fields of the sample is a small fraction of 2π over a typical domain/cluster length. The value of Φ_δ for a 1.205-\AA neutron in a $10\text{-}\mu\text{m}$ Fe domain ($B \sim 21$ kG) is ~ 1.1 rad. In the compound we are studying, the value of B is only ~ 352 G and allows Eq. (1) to be valid up to large domain sizes of about $100 \mu\text{m}$. Using the above expression, as used in the literature,³⁵ an average domain/cluster size of $\sim 5 \mu\text{m}$ is obtained at 15 K. Here the domain size is estimated by assuming a homogeneous magnetic state. However, a phase segregation in the present system, as observed in other perovskites cannot be ruled out. If the ferromagnetic domains represent only a certain volume percentage of the sample, the estimate of domain size will be different. Inaccuracy (if any) arising from the assumption of the presence of only one type of domain size can be handled by measuring the wavelength dependence of transmitted neutron beam polarization $P(\lambda)$.^{47,48} Another factor, which probably introduces an error to the estimated value of Δ is the internal mean induction B . Further uncertainty in the Δ value could arise from the assumptions of the domain structure model used here, and a full three-dimensional polarization analysis⁴⁹ would be useful in this regard. Hence, the inferred domain size of about $5 \mu\text{m}$ is meant to only reflect the order of magnitude.

In order to compare the temperature dependence of P_f with the temperature dependence of the low-field magnetization we have plotted $-\ln[P_f(T)/P_i]$ and $S[M(T)]^2$ (where S is a normalization factor) in Fig. 6(b). It is interesting to note that a temperature-independent behavior of M and P_f is evident at $T < 28$ K, indicating a temperature-independent domain size Δ below this temperature. At low applied field (50

Oe) the temperature-dependent magnetization and P_f almost overlap whereas, at higher applied fields (say 500 Oe), there is a considerable deviation between the two over the temperature range $\sim 30\text{--}90$ K. The observed variation of temperature-dependent magnetization with field revealed the field-induced magnetic ordering as observed in other perovskites.^{35,45}

We now turn to the temperature dependence of the polarization of transmitted neutron beam for the $x=0.347$ sample shown in Fig. 6(a). P_f starts decreasing below about 47 K. At $T > 47$ K, the value of P_f is the same as the incident-beam polarization. This implies that the sample is in its paramagnetic phase above 47 K where no change of neutron polarization is expected. The magnetic ordering temperature for this sample is thus estimated to be 47 K in accordance with the ac susceptibility data in Fig. 1 where a cusplike peak is found. Below 47 K depolarization data show the presence of magnetic clusters on mesoscopic length scale. At this stage, we may recall that in the zero-field cooled virgin dc magnetization data no evidence for spontaneous magnetization was found for the $x=0.347$ sample (Fig. 3). The present $x=0.347$ compound is therefore similar to the ‘‘insulator spin-glass’’ ($\text{La}_{2/3}\text{Tb}_{1/3})_{2/3}\text{Ca}_{1/3}\text{MnO}_3$ compound studied by Teresa *et al.*⁴³ where a cluster-spin-glass state with no spontaneous magnetization was found. During the passage of polarized neutrons through such a spin cluster if the Larmor precession time of neutron spins is shorter than the relaxation time τ for the clusters, the neutron spins will effectively see a nonzero precession field, and depolarization of neutron spins occurs.⁴⁵ As mentioned before, if the Larmor precession angle of the neutron spin is a small fraction of 2π over a cluster length, the observed depolarization can be represented by Eq. (1). A cluster-spin-glass state at $T < 46.5$ K is therefore confirmed for the $x=0.347$ sample. The observed characteristic temperature dependency of χ_{ac} for the $x=0.347$ sample indicates the cluster-spin-glass freezing. We may recall that according to the phase diagram given by Terai *et al.*,³⁸ the $x=0.347$ sample ($t=0.905$) belongs to an insulator-spin-glass. The $x=0.347$ compound remains an insulator within the limits of our measurements. It is important to stress that the observed cluster-spin-glass behavior for the $x=0.347$ sample occurs within the insulating phase as opposed to the fact that for manganites, the DE-mediated insulating spin-glass phase should be of canonical (true) type. The $x=0.347$ compound is therefore in a double-exchange-mediated insulating cluster-spin-glass state, as observed for example in the case of $(\text{La}_{2/3}\text{Tb}_{1/3})_{2/3}\text{Ca}_{1/3}\text{MnO}_3$ ^{40,41,43} where a significant increase in the low-angle magnetic neutron scattering was found at $T \leq 95$ K, indicating the presence of spin clusters and a very steep rise in resistivity below 150 K.

F. Crystal structure and magnetic ordering

When Dy^{3+} replaces La^{3+} , during doping, the $\text{Mn}^{3+}/\text{Mn}^{4+}$ ratio remains fixed at its original value of 7/3 as in the $\text{La}_{0.7}\text{Ca}_{0.3}\text{MnO}_3$ parent compound and, hence, the number of mobile e_g electrons and also the number of available hopping sites for the e_g electrons (responsible for double-exchange interaction) remains fixed. However, dop-

ing of La^{3+} ions (ionic radius: 1.216 Å) by smaller Dy^{3+} ions (ionic radius: 1.083 Å)⁶³ is expected to alter the hopping integral for the mobile e_g electrons as mentioned in the Introduction. Microscopic distortion in perovskite structure of the manganites can be quantified by the geometrical tolerance factor t , defined as $t = (r_A + r_O) / \sqrt{2}(r_{\text{Mn}} + r_O)$, where r_A is the average ionic radius of R^{3+} and Ca^{2+} , r_O is the ionic radius of O^{2-} , and r_{Mn} is the average ionic radius of Mn^{3+} and Mn^{4+} . In an ideal, undistorted perovskite structure with cubic symmetry ($t=1$), the value of the Mn-O-Mn bond angle (with the manganese ions being octahedrally coordinated to the oxygen ions) is 180 deg. With a decrease in the value of t from its ideal value of “unity,” the Mn-O-Mn bond angle reduces, distorting the structure first to rhombohedral symmetry involving cooperative rotation of the MnO_6 octahedra about the [111] axis and then to orthorhombic symmetry with GdFeO_3 -type structure (as found for the present compounds), involving cooperative rotation about the [110] axis. As expected from the sizes of the La^{3+} and the Dy^{3+} ions, the tolerance factor (t) values in the present case, calculated using ionic radii reported by Shannon,⁶³ shows a decreasing trend with increasing Dy concentration ($t=0.916, 0.913, 0.908$, and 0.905 for $x=0, 0.114, 0.243$, and 0.347 , respectively). This gives an increase in the buckling of MnO_6 causing a decrease in the Mn-O-Mn bond angle further below 180 deg (Ref. 39) and subsequent narrowing down of the one-electron bandwidth W of the e_g electrons.³⁷ This causes a decrease in the transfer integral t_o , which in turn, weakens DE (ferromagnetic) interaction and thus explains qualitatively the deterioration of the observed ferromagnetic and conducting properties. A strong competition between the coexisting ferromagnetic DE interactions and $t_{2g}(\text{Mn})-2p_\pi(\text{O})-t_{2g}(\text{Mn})$ antiferromagnetic superexchange interaction in the highly distorted structures gives rise to magnetically disordered states with canted ferromagnetic metallic state for the $x=0.243$ compound and a cluster-spin-glass insulating state for the $x=0.347$ compound. The electronic and magnetic properties of manganites depend not only on the tolerance factor, but also on the variance (second moment, a parameter corresponding to a random distribution of Mn-O-Mn bond angles) σ^2 defined by the equation $\sigma^2 = y_i r_i^2 - r_A^2$, where r_i is the radius of each R^{3+} and A^{2+} , y_i is the fractional occupancies of the i ions ($\sum y_i = 1$), r_A is the average ionic radius of R^{3+} and A^{2+} ions.^{42,44,64,65} A contribution due to random distribution of Mn-O-Mn bond angles towards the spin-glass transition has also been discussed in Ref. 44. The role played by the intrinsic disorder in these mixed-valent systems has also been underlined^{65,66} in the context of the inhomogeneous states found on various scales from the formation of polaronic clusters or clustered magnetic regions⁶⁷ up to large-scale phase separation.^{68,69} σ^2 of $(\text{La}_{1-x}\text{Dy}_x)_{0.7}\text{Ca}_{0.3}\text{MnO}_3$ increases with increasing Dy^{3+} content.³⁸ A large value of σ^2 corresponds to a random distribution of the Mn-O-Mn bond angles (closely related to the transfer integral), makes the specimen magnetically inhomogeneous, and drives the system towards the spin-glass state.

IV. SUMMARY AND CONCLUSION

Using ac susceptibility, dc magnetization, resistivity, neutron-depolarization, and neutron-diffraction techniques,

we have investigated the A-site (La-site) ionic size effect on the magnetic ordering in $\text{La}_{0.7-x}\text{Dy}_x\text{Ca}_{0.3}\text{MnO}_3$ (with $x=0, 0.114, 0.243$, and 0.347). In the $x=0$ (parent) and 0.114 compounds, there is clear evidence of long-range ferromagnetic order in the low-temperature metallic state, due to ordering of Mn spins, as revealed by the low-temperature neutron-diffraction experiments. Our neutron-diffraction study also shows that the Dy site is not magnetically ordered down to 9 K, the lowest temperature of our measurements. For the $x=0.243$ sample, the spontaneous magnetization is found to be quite low to show any observable intensity in the neutron diffraction pattern in its low temperature metallic state. However, the neutron-depolarization study confirms the existence of quite large ($\sim 5 \mu\text{m}$) ferromagnetic domains with low net magnetic moments below 65 K. It is, therefore, suggested that the spins are highly canted in the $x=0.243$ compound causing the randomly canted ferromagnetic phase with average canting angle Φ of Mn spins ≥ 82 deg. The canting of Mn spins occurs due to the competition between the antiferromagnetic and reduced ferromagnetic interactions with lowering of tolerance factor and with increase in disorder caused by the random substitution of Dy ions at the La sites. For higher degree of Dy substitution ($x=0.347$) spin clusters have been observed at lower temperature. The magnetic and transport behavior of the present $x=0.347$ compound is similar to that of the “insulator spin-glass” $(\text{La}_{2/3}\text{Tb}_{1/3})_{2/3}\text{Ca}_{1/3}\text{MnO}_3$ compound studied by Teresa *et al.*⁴³ The spin-cluster behavior of the $x=0.347$ sample seems to come from a more detailed balance of competing ferromagnetic and antiferromagnetic interactions and also due to disorder. Remaining magnetic coupling of the clusters leads to a cluster-spin-glass-like behavior. The electrical resistivity measurement shows that the $x=0.347$ sample remains an insulator in its cluster spin-glass state. A broad distribution of cluster sizes is probable in the $x=0.347$ sample. Small-angle neutron-scattering³⁴ and wavelength-dependent neutron-depolarization study^{47,48} may give a quantitative measure of the size distribution of these clusters. We must mention that we have assumed all along a homogeneous magnetic state model, although phase segregation as observed in other perovskites cannot be ruled out.

Microscopically, the effects of the Dy substitution can be understood as follows: With increasing Dy concentration, the tolerance factor t ($=0.916, 0.913, 0.908$, and 0.905 for $x=0, 0.114, 0.243$, and 0.347 , respectively) decreases. This causes a bending of Mn-O-Mn bonds away from 180 deg and gives weaker transfer integral t_o for the hopping of e_g electrons. Reduction in the Mn-O-Mn bond angles leads to narrower one-electron bandwidth. The narrow bandwidth effectively reduces the transfer integral of e_g electrons, thereby favoring an insulating state. This, in turn, gives weaker DE interaction, resulting in the reduction of ferromagnetic exchange. Consequently, DE ferromagnetic interactions and coexisting $t_{2g}(\text{Mn})-2p_\pi(\text{O})-t_{2g}(\text{Mn})$ antiferromagnetic superexchange interactions compete more strongly depending on the structural distortion, giving rise to a magnetically disordered state. The electronic and magnetic properties of manganites depend not only on the tolerance factor but also on the variance (second moment, a parameter corresponding to

a random distribution of Mn-O-Mn bond angles) σ^2 . The σ^2 of $(\text{La}_{1-x}\text{Dy}_x)_{0.7}\text{Ca}_{0.3}\text{MnO}_3$ increases with increasing Dy^{3+} content.³⁸ A large value of σ^2 corresponds to a random distribution of the Mn-O-Mn bond angles (closely related to the transfer integral), making the specimen magnetically inhomogeneous and drives the system towards a spin-glass state.

Randomly canted ferromagnetic state (in $\text{La}_{0.67}\text{Ca}_{0.33}\text{Mn}_{0.9}\text{M}_{0.1}\text{O}_3$, $M = \text{Fe},^{35} \text{Ga},^{45}$) and cluster spin-glass state [in $\text{La}_{2/3}\text{Ca}_{1/3}\text{Mn}_{1-x}\text{T}_x\text{O}_3$, $T = \text{In},^{29} \text{Ti},^{24} \text{Al},^{28}$ and $(\text{La}_{1-x}\text{Tb}_x)_{2/3}\text{Ca}_{1/3}\text{MnO}_3$, (Refs. 41 and 43)] have already been reported for several Mn- and La-site doped manganites. The present magnetic and transport studies on the $(\text{La}_{1-x}\text{Dy}_x)_{0.7}\text{Ca}_{0.3}\text{MnO}_3$ compounds, however, give a clearer understanding about the evolution of the length scale of magnetic ordering in the ferromagnetic manganites with a decrease in the average size of the ions at the rare-earth site. Since in the present Dy substituted systems, the $\text{Mn}^{3+}/\text{Mn}^{4+}$ ratio remains fixed at its original value of 7/3 as in the $\text{La}_{0.7}\text{Ca}_{0.3}\text{MnO}_3$ parent compound (and hence the number of mobile e_g electrons and also the number of available hopping sites for the e_g electrons, responsible for double-exchange interaction, remain unchanged) and there is no ordered moment on Dy ions down to the lowest temperature studied, all the observed effects can be ascribed to a pure lattice effect as influenced by the change in the tolerance factor value. Unlike the several magnetic phase diagrams published so far on the effect of the lattice on the magnetic properties of the manganites,^{37,38,41,43} the present work,

which includes the results of a neutron-depolarization study, gives a robust demonstration of the existence of ferromagnetic domains in the canted ferromagnetic state of the $x = 0.243$ compound and spin clusters in the cluster-spin-glass state of the $x = 0.347$ compound. There is no breakdown of ferromagnetic domain structure in the $x = 0.243$ compound, down to the lowest temperature (covering the temperature range where resistivity shows an upturn, indicating a reentrant transition to an insulating behavior), as opposed to what was concluded earlier by Terai *et al.*³⁸ The randomly canted ferromagnetic state of this compound is somewhat similar to that in $\text{La}_{0.67}\text{Ca}_{0.33}\text{Mn}_{0.9}\text{Fe}_{0.1}\text{O}_3$,³⁵ where a sizable frustrated antiferromagnetic superexchange involving Fe^{3+} ions was present. It may be recalled that the phase diagram given by Terai *et al.*³⁸ for the same series $(\text{La}_{1-x}\text{Dy}_x)_{0.7}\text{Ca}_{0.3}\text{MnO}_3$ indicates a spin-glass insulating phase when t is smaller than 0.907. It was concluded³⁸ that the spin-glass insulator in $(\text{La}_{1-x}\text{Dy}_x)_{0.7}\text{Ca}_{0.3}\text{MnO}_3$, for $t < 0.907$, is different from a ferromagnetic insulator that appears in the compounds containing light rare-earth metal ions³⁷ of Pr^{3+} and/or Y^{3+} . However, our study shows that even for Dy concentration as high as 0.347 ($t = 0.905$) a cluster-spin-glass state persists. Comparing with rare-earth doped manganites such as in $\text{Gd}_{0.67}\text{Ca}_{0.33}\text{MnO}_3$,⁷⁰ where the rare-earth site was reported to order magnetically, we find no evidence for any magnetic ordering of Dy down to 9 K. Our experimental results, therefore, essentially reflect how $\langle r_R \rangle$ and σ of the La sublattice influence the magnetic order at different length scales.

*Corresponding author. FAX: +91-22-25505151 Electronic address: smyusuf@apsara.barc.ernet.in

[†]Present address: International Atomic Energy Agency, Vienna, Austria.

¹S. Jin, T.H. Tiefel, M. McCormack, R.A. Fastnacht, R. Ramesh, and L.H. Chen, *Science* **264**, 413 (1994).

²R.V. Helmolt, J. Wecker, B. Holzapfel, L. Schultz, and K. Samwer, *Phys. Rev. Lett.* **71**, 2331 (1993).

³R. Mahesh, R. Mahendiran, A.K. Raychudhuri, and C.N.R. Rao, *J. Solid State Chem.* **114**, 297 (1995).

⁴E.O. Wollan and W.C. Koehler, *Phys. Rev.* **100**, 545 (1955).

⁵P. Schiffer, A.P. Ramirez, W. Bao, and S.-W. Cheong, *Phys. Rev. Lett.* **75**, 3336 (1995).

⁶Y. Tomioka, A. Asamitsu, Y. Moritomo, H. Kuwahara, and Y. Tokura, *Phys. Rev. Lett.* **74**, 5108 (1995).

⁷K. Liu, X.W. Wu, K.H. Ahn, T. Sulchek, C.L. Chien, and J.Q. Xiao, *Phys. Rev. B* **54**, 3007 (1996).

⁸A. Asamitsu, Y. Moritomo, Y. Tomioka, T. Arima, and Y. Tokura, *Nature (London)* **373**, 407 (1995).

⁹A.J. Campbell, G. Balakrishnan, M.R. Lees, D.McK. Paul, and G.J. McIntyre, *Phys. Rev. B* **55**, 8622 (1997).

¹⁰H. Kuwahara, Y. Tomioka, A. Asamitsu, Y. Moritomo, and Y. Tokura, *Science* **270**, 961 (1995).

¹¹C. Zener, *Phys. Rev.* **82**, 403 (1951).

¹²J. Töpfer and J.B. Goodenough, *Chem. Mater.* **9**, 1467 (1997).

¹³F.K. Lotgering, *Philips Res. Rep.* **25**, 8 (1970); J.B.A.A. Elemans, B. van Laar, K.R. van der Veen, and B.O. Loopstra, *J. Solid State Chem.* **3**, 238 (1971).

¹⁴L.K. Leung, A.H. Morrish, and B.J. Evans, *Phys. Rev. B* **13**, 4069

(1976); L.K. Leung and A.H. Morrish, *ibid.* **15**, 2485 (1977).

¹⁵E.P. Svirina, L.P. Shlyakhina, and F.F. Shakirova, *Sov. Phys. Solid State* **30**, 2129 (1988); **32**, 557 (1990).

¹⁶M. Rubinstein, D.J. Gillespie, J.E. Snyder, and T.M. Tritt, *Phys. Rev. B* **56**, 5412 (1997).

¹⁷G. Turilli and F. Licci, *Phys. Rev. B* **54**, 13052 (1996).

¹⁸Y. Sun, Xu Xiaojun, Lei Zheng, and Y. Zhang, *Phys. Rev. B* **60**, 12 317 (1999).

¹⁹J. Gutiérrez, A. Peñna, J.M. Barandiarán, T. Hernández, L. Lezama, M. Insausti, and T. Rojo, *Phys. Rev. B* **61**, 9028 (2000).

²⁰N. Gayathri, A.K. Raychudhuri, S.K. Tiwary, R. Gundakaram, A. Arulraj, and C.N.R. Rao, *Phys. Rev. B* **56**, 1345 (1997).

²¹R.K. Sahu, Q. Mohammad, M.L. Rao, S.S. Manoharan, and A.K. Nigam, *Appl. Phys. Lett.* **80**, 88 (2002).

²²C. Osthöver, P. Grünberg, and R.R. Arons, *J. Magn. Magn. Mater.* **177-181**, 854 (1998).

²³K.H. Ahn, X.W. Wu, K. Liu, and C.L. Chien, *Phys. Rev. B* **54**, 15 299 (1996).

²⁴X. Liu, X. Xu, and Y. Zhang, *Phys. Rev. B* **62**, 15 112 (2000).

²⁵M. Sahana, K. Dörr, M. Doerr, D. Eckert, K.-H. Müller, K. Nenkov, L. Schultz, and M.S. Hegde, *J. Magn. Magn. Mater.* **213**, 253 (2000).

²⁶R. von Helmholt, L. Haupt, K. Bärner, and U. Sondermann, *Solid State Commun.* **82**, 693 (1992); L. Haupt, R. von Helmholt, U. Sondermann, K. Bärner, Y. Tang, E.R. Giessinger, E. Ladizinsky, and R. Braunstein, *Phys. Lett. A* **165**, 473 (1992).

²⁷A. Maignan, C. Martin, and B. Raveau, *Z. Phys. B: Condens. Matter* **102**, 19 (1997).

²⁸J. Blasco, J. García, J.M. De Teresa, M.R. Ibarra, J. Perez, P.A.

- Algarabel, C. Marquina, and C. Ritter, *Phys. Rev. B* **55**, 8905 (1997).
- ²⁹M.C. Sanchez, J. Blasco, J. García, J. Stankiewicz, J.M. De Teresa, and M.R. Ibarra, *J. Solid State Chem.* **138**, 226 (1998).
- ³⁰J.R. Sun, G.H. Rao, B.G. Shen, and H.K. Wong, *Appl. Phys. Lett.* **73**, 2998 (1998); I.V. Medvedeva, K. Bärner, G.H. Rao, N. Hamad, Yu.S. Bersenev, and J.R. Sun, *Physica B* **292**, 250 (2000).
- ³¹J.L. Alonso, L.A. Fernández, F. Guinea, V. Laliena, and V. Martín-Mayor, cond-mat/0111244 (unpublished).
- ³²M.X. Xu and Z.K. Jiao, *J. Mater. Sci. Lett.* **18**, 1307 (1999).
- ³³Jian-Wang Cai, Cong Wang, Bao-Gen Shen, Jian-Gao Zhan, and Wen-Shan Zhan, *Appl. Phys. Lett.* **71**, 1727 (1997).
- ³⁴A. Simopoulos, M. Pissas, G. Kallias, E. Devlin, N. Moutis, I. Panagiotopoulos, D. Niarchos, C. Christides, and R. Sonntag, *Phys. Rev. B* **59**, 1263 (1999).
- ³⁵S.M. Yusuf, M. Sahana, M.S. Hegde, K. Dörr, and K.-H. Müller, *Phys. Rev. B* **62**, 1118 (2000).
- ³⁶R.S. Freitas, L. Ghivelder, F. Damay, F. Dias, and L.F. Cohen, *Phys. Rev. B* **64**, 144404 (2001).
- ³⁷H.Y. Hwang, S.-W. Cheong, P.G. Radaelli, M. Marezio, and B. Batlogg, *Phys. Rev. Lett.* **75**, 914 (1995).
- ³⁸T. Terai, T. Kakeshita, T. Fukuda, T. Saburi, N. Takamoto, K. Kindo, and M. Honda, *Phys. Rev. B* **58**, 14 908 (1998).
- ³⁹S.M. Yusuf, R. Ganguly, K.R. Chakraborty, P.K. Mishra, S.K. Paranjpe, J.V. Yakhmi, and V.C. Sahni, *J. Alloys Compd.* **326**, 89 (2001).
- ⁴⁰J. Blasco, J. Garcia, J.M. De Teresa, M.R. Ibarra, P.A. Algarabel, and C. Marquina, *J. Phys.: Condens. Matter* **8**, 7427 (1996).
- ⁴¹J.M. De Teresa, C. Ritter, M.R. Ibarra, P.A. Algarabel, J.L. Garcia-Munoz, J. Blasco, J. Garcia, and C. Marquina, *Phys. Rev. B* **56**, 3317 (1997).
- ⁴²L.M. Rodriguez-Martinez and J.P. Attfield, *Phys. Rev. B* **54**, R15 622 (1996).
- ⁴³J.M. De Teresa, M.R. Ibarra, J. Garcia, J. Blasco, C. Ritter, P.A. Algarabel, C. Marquina, and A. del Moral, *Phys. Rev. Lett.* **76**, 3392 (1996).
- ⁴⁴T. Terai, T. Sasaki, T. Kakeshita, T. Fukuda, T. Saburi, H. Kitagawa, K. Kindo, and M. Honda, *Phys. Rev. B* **61**, 3488 (2000).
- ⁴⁵S.M. Yusuf, M. Sahana, K. Dörr, U.K. Röbber, and K.-H. Müller, *Phys. Rev. B* **66**, 064414 (2002).
- ⁴⁶G. Halperin and T. Holstein, *Phys. Rev.* **59**, 960 (1941).
- ⁴⁷S. Mitsuda and Y. Endoh, *J. Phys. Soc. Jpn.* **54**, 1570 (1985).
- ⁴⁸I. Mirebeau, S. Itoh, S. Mitsuda, T. Watanabe, Y. Endoh, M. Hennion, and P. Calmettes, *Phys. Rev. B* **44**, 5120 (1991).
- ⁴⁹R. Rosman, Ph.D. thesis, Delft University of Technology, 1991.
- ⁵⁰S.M. Yusuf and L. Madhav Rao, *Neutron News* **8**, 12 (1997).
- ⁵¹S.M. Yusuf and L. Madhav Rao, *Pramana, J. Phys.* **47**, 171 (1996).
- ⁵²L. Madhav Rao, S.M. Yusuf, and R.S. Kothare, *Indian J. Pure Appl. Phys.* **30**, 276 (1992).
- ⁵³S.K. Paranjpe and Y.D. Dande, *Pramana* **32**, 793 (1989).
- ⁵⁴Q. Huang, A. Santoro, J.W. Lynn, R.W. Erwin, J.A. Borchers, J.L. Peng, K. Ghosh, and R.L. Greene, *Phys. Rev. B* **58**, 2684 (1998).
- ⁵⁵X.L. Wang, J. Horvat, H.K. Liu, and S.X. Dou, *Solid State Commun.* **108**, 661 (1998).
- ⁵⁶J. Rodriguez-Carvajal, computer code FULLPROF, version 3.0.0 Laboratoire Leon Brillouin, CEA-CNRS, 1995.
- ⁵⁷A. Das, M. Sahana, S.M. Yusuf, L. Madhav Rao, C. Shivakumara, and M.S. Hegde, *Mater. Res. Bull.* **35**, 651 (2000).
- ⁵⁸P.-G. De Gennes, *Phys. Rev.* **118**, 141 (1960).
- ⁵⁹C. Mitra, P. Raychaudhuri, S.K. Dhar, A.K. Nigam, R. Pinto, and S.M. Pattalwar, *J. Magn. Magn. Mater.* **192**, 130 (1999).
- ⁶⁰S.M. Yusuf, L. Madhav Rao, P.L. Paulose, and V. Nagarajan, *J. Magn. Magn. Mater.* **166**, 349 (1997).
- ⁶¹I. Mirebeau, S. Itoh, S. Mitsuda, T. Watanabe, Y. Endoh, M. Hennion, and R. Papoulet, *Phys. Rev. B* **41**, 11 405 (1990).
- ⁶²R. Erwin, *J. Appl. Phys.* **67**, 5229 (1990).
- ⁶³R.D. Shannon, *Acta Crystallogr., Sect. A: Cryst. Phys., Diffr., Theor. Gen. Crystallogr.* **32**, 751 (1976).
- ⁶⁴F. Damay, C. Martin, A. Maignan, and B. Raveau, *J. Appl. Phys.* **82**, 6181 (1997).
- ⁶⁵C. Martin, A. Maignan, M. Hervieu, and B. Raveau, *Phys. Rev. B* **60**, 12 191 (1999).
- ⁶⁶A. Moreo, M. Mayr, A. Feiguin, S. Yunoki, and E. Dagotto, *Phys. Rev. Lett.* **84**, 5568 (2002); E. Dagotto, T. Hotta, and A. Moreo, *Phys. Rep.* **344**, 1 (2001).
- ⁶⁷J.M. De Teresa, M.R. Ibarra, P.A. Algarabel, C. Ritter, C. Marquina, J. Blasco, J. Garcia, A. Del Moral, and Z. Arnold, *Nature (London)* **386**, 256 (1997).
- ⁶⁸M. Uehara, S. Mori, C.H. Chen, and S.-W. Cheong, *Nature (London)* **399**, 560 (1999); M. Fäth, S. Freisem, A.A. Menovsky, Y. Tomioka, J. Aarts, and J.A. Mydosh, *Science* **285**, 1540 (1999).
- ⁶⁹E.E. Narimanov and C.M. Varma, *Phys. Rev. B* **64**, 024429 (2001); B.M. Letfulov and F.K. Freericks, *ibid.* **64**, 174409 (2001); M. Auslender and E. Kogan, *ibid.* **64**, 012408 (2001); N. Shannon and A.V. Chubukov, *J. Phys.: Condens. Matter* **14**, L235 (2002).
- ⁷⁰G.J. Snyder, C.H. Booth, F. Bridges, R. Hiskes, S. DiCarolis, M.R. Beasley, and T.H. Geballe, *Phys. Rev. B* **55**, 6453 (1997).